Decomposition of Ferrocene on Pt(111) and its Effect on Molecular Electronic Junctions

Jeffrey R. Reimers,[#$*] Yin Wang,[#] and Daniel S. Kosov[&*]

International Centre for Quantum and Molecular Structures and the School of Physics, Shanghai University, Shanghai 200444, China

$ School of Mathematical and Physical Sciences, University of Technology Sydney, Sydney NSW 2007, Australia

& College of Science and Engineering, James Cook University, Townsville, QLD 4811, Australia.

Supporting Information Placeholder

ABSTRACT: From dilute vapor, ferrocene encountering Pt(111) decomposes, producing bound cyclopentadienyl rings, in contrast to its legendary stability in solution electrochemistry. We propose that decomposition occurs through initial chemisorption, making a Pt-C bond to a ferrocenium hydride, followed by step-edge catalyzed decomposition leading to migration of the Fe atom inside the Pt bulk. These conclusions are based on results from density-functional theory (DFT) calculations. When Pt(111) approaches ferrocene tethered to a self-assembled monolayer, only the first, spontaneous but mechanically reversible, chemisorption is predicted when Pt(111). Non-equilibrium Green's function calculations utilizing DFT predict that chemisorption increases molecular-junction conductivities by a factor of 2-5. This could contribute to the extremely high conductivities observed in junctions supporting rectification up to unprecedented high-frequency cut-offs of ~520 GHz, though squashed junctions at half monolayer coverage are predicted to conduct 10^4 times better.

INTRODUCTION

The recent observation[1] of the decomposition of low-pressure gas-phase ferrocene (Fc) on Pt(111), producing bound cyclopentadienyl (Cp) rings, stands in stark contrast to the use of Fc and Pt(111) as an IUPAC standard in solution electrochemistry.[2-4] The fate of the ferrocene iron on decomposition remains uncertain;[1] understanding the mechanism of decomposition and its wider significance presents a significant scientific challenge. Of relevance is that Fc has recently been shown to decompose flowing deposition of atoms onto it.[5] Also, Fc on Pt(111) is a particularly useful system as oxidation of the Fc adlayer produced following alternate exposure at high Fc pressures, by O_2, leads to just FeO on the surface, an adlayer with catalytic properties.[1]

In addition, particularly relevant to modern applications is the widespread use of Fc tail groups on self-assembled monolayers (SAMs) in single-molecule conductivity experiments.[6-9] This field has yielded some stunning results in recent years,[10] including junctions that continue to rectify at frequencies beyond the present limits of measurement (17 GHz), estimated to reach 520 GHz.[11] Of note, the unexplained observed[11] conductivity of these junctions is 10^4 times higher than naively expected. Related advances include similar molecular junctions with rectification ratios[12-14] of 10^3-10^5, and the development of high-yield techniques.[15] While the conditions used in molecular-electronics measurements can involve various solvents[16] or UHV, solvent and other factors are likely to be excluded as junctions close, making reactions under gas-phase conditions of general relevance. In junction, is the decomposition of Fc partially or fully completed? How does this affect conductivity?

To address these issues, calculations using density functional theory (DFT) were performed for the binding and decomposition pathways of Fc on Pt(111), as well as for the approach of Pt(111) to various alkanethiol SAMs made with Fc tail groups.[7, 11, 17-18] Also, junction conductivities are evaluated using the non-equilibrium Green's function approach combined with DFT (NEGF-DFT).[19]

METHODS

All surface equilibrium DFT calculations were performed using VASP 5.4.1,[20] with the valence electrons separated from the core (4 valence electrons for C, 6 for S, 8 for Fe, 10 for Pt, and 11 for Au) using projector-augmented wave pseudopotentials (PAW).[21] The energy cut-off for the plane-wave basis functions was determined using the "PREC = NORMAL" command, except for vibrational frequency calculations which used "PREC = HIGH" instead. A cutoff of 402.4 eV is used for the plane-wave basis set in all calculations. The energy tolerance for the electronic structure determinations was set at 10^{-7} eV to ensure accuracy, with geometry optimizations converged to a tolerance of 0.02 eV $Å^{-1}$. The Perdew, Burke, and Ernzerhof (PBE)[22] functional is used, augmented by Grimme's "D3(BJ)" dispersion correction.[23] Optimized coordinates for all structures described are provided in Supporting Information (SI).

For Fc reacting with Pt(111), a $(7\times2\sqrt{3})$R30° surface cell was used at $R_{Pt\text{-}Pt}$ = 2.772 Å, along with a **k**-space grid of 1×2×1. The Pt slab was four 28-atom layers thick, with 12 atoms per cell in a 3-atom wide stripe forming part of a 5th layer so as to manifest a step edge, see Fig. 1. A vacuum region of ca. 20 Å separated slabs from each other. For Fc-terminated SAMs approaching Pt(111), a gold substrate was used to which a ferrocenyl undecan-

ethiol SAM[11, 17-18] at low coverage (1:24) was tethered. A commensurate (6×2√3)R30° surface cell was used with $R_{Pt\text{-}Pt} = R_{Au\text{-}Au}$ = 2.884 Å. A **k**-space grid of 1×2×1 was used, with the cell height set to 35 Å.

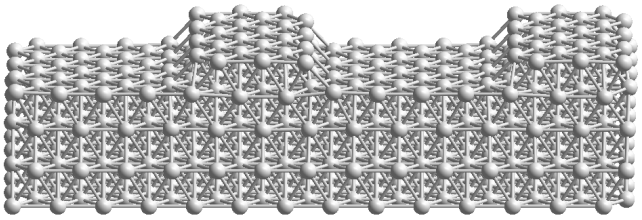

Figure 1. A 2×2 replica of the (7×2√3)R30° Pt(111) surface with step edge, used to model the reaction between Pt(111) and Fc.

Junction conductivity calculations were performed by a DFT-based NEGF method[19] using NANODCAL.[19, 24] The molecular wire junction was divided into three regions, left electrode, contact region, and right electrode. DFT with the PBE functional[22] was used to construct a single-particle Hamiltonian for NEGF electron transport calculations. We used double-zeta with polarization basis set, **k**-space grids of 2×3×1, and 80 a.u. energy cutoff for real-space grid in all electron transport calculations.

RESULTS AND DISCUSSION

Ferrocene decomposition on Pt(111). Figure 2 depicts key structures, mostly local-minima and transition states, encountered along a continuous, arbitrarily chosen, path linking the isolated surface and Fc to dissociated products. The individual activation energies for each step are at most 0.8 eV (18 kcal mol^{-1}) , suggesting that they should be rapid on the time scale used in the experiments.[1]

The calculations indicate, at low coverage, that Fc can bind physisorbed in a π-stacked geometry **1** or else approach perpendicular to this, through **2** and barrierlessly on to the chemisorbed structure **3**. On a flat surface, the calculations predict that the chemisorbed structure is 0.2 eV more stable than the physisorbed one, though near a step edge (Fig. 2) their relative energies are similar. While possible errors in these calculations could be of order 0.2 eV, the calculated barrier for rotation from **1** to **2** is low, a feature expected to be a robust prediction, indicating that **2** should be easily accessible at room temperature.

Formation of **3** is a chemisorption process in which a Pt-C bond forms, with the CH hydrogen shifting to bind to the iron to make a ferrocenium hydride. This hydrogen goes on to catalyze later reactions; in Fig. 2, hydrogens are shown in black to highlight their location. Subsequently, this hydrogen can shift to a different local-minimum structure **4** in which it bridges Fe to Pt, and then on to **5** in which it binds purely to the surface. The chemisorbed Fc and its nearby hydrogen can then migrate across the surface via **6** and **7** until they reach a step edge.

In the path followed, the hydrogen then mounts the surface **8**, rebinding to the Fe, **9**, to open the Fc sandwich and allow the top Cp ring to π-stack to the Pt(111) edge top, **10**. During this, the Fe atom moves towards a Pt(111) FCC site adjacent to the step edge. Next, the lower Cp ring dissociates from the Fe, sitting upright on the surface **11**. Toppling over, **12** provides a transition state leading to the deeply bound structure **13**. Low barrier migration of the hydrogen from the step edge **14** then leads to the transition state **15** for recombination of the hydrogen with the Cp ring, **16**. This structure, at an energy of -3.89 eV relative to the separated Fc and surface, is the lowest-energy structure found in the calculations. However, the top Cp ring still hovers over the Fe. In search of fully dissociated products, we force this Cp to slide over the transition state **17** to yield **18**. This structure is only 0.23 eV less stable than the step-edge bound intermediate **16**; they will be favored by entropy, and will be driven by expected large effective molarity of Fc approaching the step edge.

The described path in Fig. 2 serves only to demonstrate the feasibility of step-edge decomposition at room temperature, and many lower-energy or kinetically more favored paths may be available. Indeed, many other structures were found in the calculations through which no continuous path was obtained, but we do report in Fig. 2 the lowest-energy trap sites found for the different stages of decomposition. A key feature of the results is that the migrating hydrogen atom can move freely across the surface at many stages of the process. Its independent recombination from **13** to **16** is unintuitive, however, as other processes could consume the freely translating atom. We found structures similar to **9** in which the hydrogen bridged C to Fe as in **3**, but searches for direct one-step paths from them to **16** were unsuccessful.

The experiments concerning Fc exposure to Pt(111) at low pressure show surfaces covered by Cp, without determining the fate of the dissociated Fe atoms.[1] X-ray photoelectron spectroscopy (XPS) failed to see any Fe(2p) signal and scanning-tunneling microscopy (STM) images showed no features interpretable as surface Fe. We performed some cluster calculations using Gaussian-16[25] for Fe in its environment in **16** (B3LYP density functional[26] with the 6-31G* basis set[27] for Fe and LANL2DZ[28] for Pt). These predict that if Fe atoms remain bound to step edges then a Fe(2p) signal should indeed have been observed by the XPS experiments. It has been postulated that the iron evaporates from the surface as FeCp.[1] We investigate this and other possibilities for Fe loss, evaluating overall energy changes for the reactions:

Pt(111)+Fc →	Pt(111).Cp+^{4}FeCp	ΔE = 2.37 eV,
	Pt(111).C_5H_4+^{5}HFeCp	ΔE = 2.50 eV,
	Pt(111).C_5H_4+^{3}FeC_5H_6	ΔE = 3.76 eV,
	Pt(111).2Cp+^{5}Fe	ΔE = 1.44 eV,
	Pt(111).2C_5H_4+^{5}FeH_2	ΔE = 4.15 eV.

Reaction energies are listed only for the predicted lowest-energy product spin state, with the step-edge model (Fig. 1) used for the Pt(111) surface. All of these reactions involving Fe loss are predicted to be endothermic, with the lowest-energy process, dissociation of bare Fe atoms, being 5.3 eV (120 kcal mol^{-1}) in energy above the bound species **18**. Hence desorption of the Fe appears to be extremely unlikely.

Loss of Fe XPS and STM signals could also be explained by migration of Fe atoms from structures like **18** into the bulk platinium.[1] Swapping the Fe atom in **18** with Pt atoms in the two rows below it produces structures **19** and **20** in Fig. 3, with conversion to **20** predicted to be exothermic by 0.1 eV. Hence the most likely explanation of the observed loss in Fe signal is Fe diffusion into the bulk metal, perhaps assisted by local heating resulting from the large exothermicity of the ferrocene decomposition reaction.

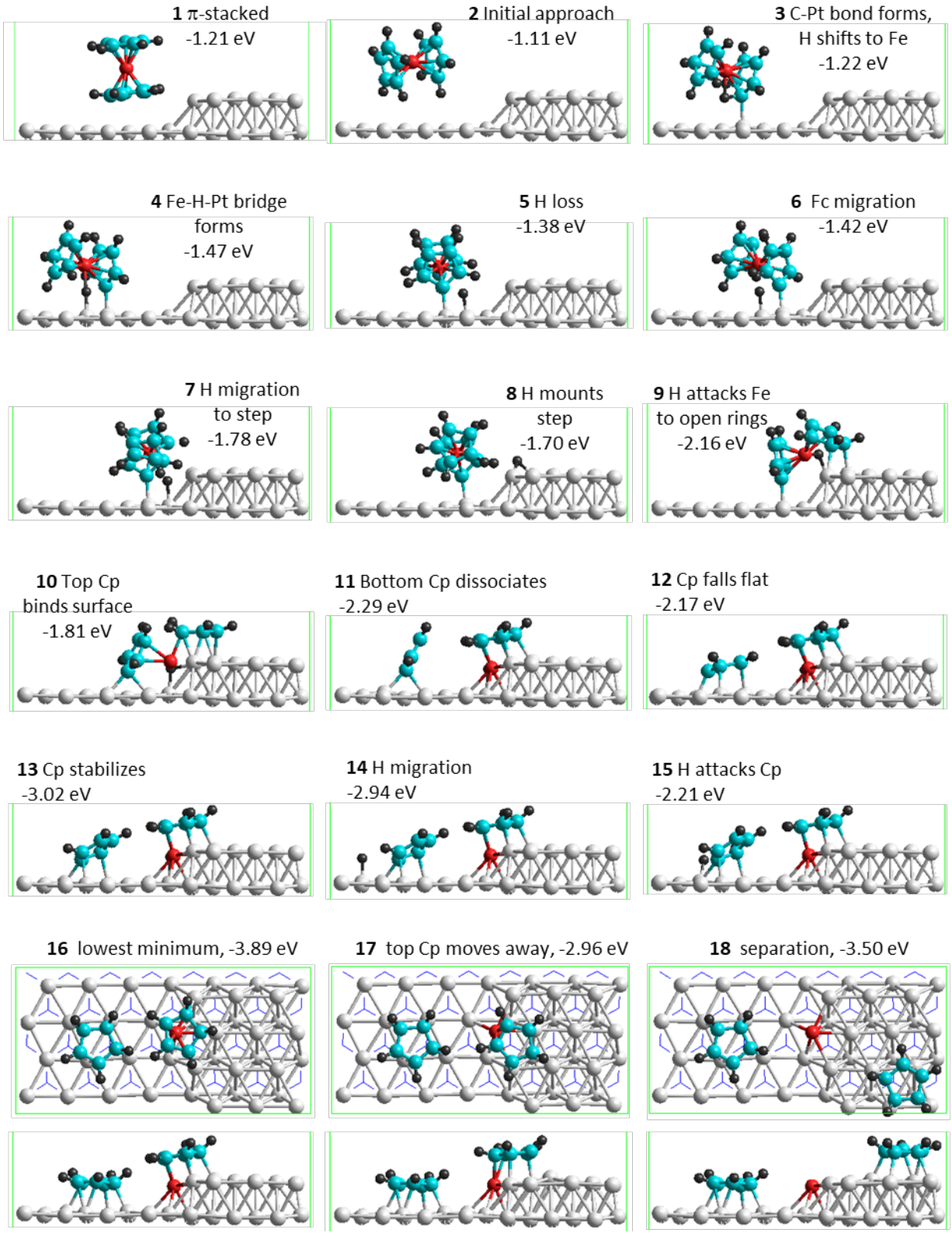

Figure 2. A continuous reaction pathway depicting a viable process at 298 K for the rapid decomposition of Fc on Pt(111), from DFT calculations. All structures are local minima except for the intermediate **2** and the transition states **12**, **15**, and **17**. Energies ΔE are listed relative to that for the isolated surface and Fc molecule. Pt- white, Fe- red, C- cyan, H- black, unit-cell vectors- green; in the top views shown in addition for **16** - **18**, subsurface-layer Pt are indicated in blue.

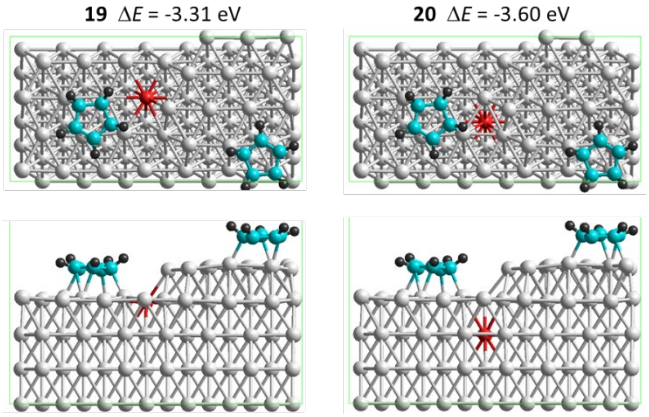

Figure 3. Some structures in which **18** is modified to interchange Fe with various Pt atoms. Pt- white, Fe- red, C- cyan, H- black, unit-cell vectors- green.

Of note too is that, using high resolution electron energy loss spectroscopy (HREELS), vibrational frequencies of Fc and Cp on Pt(111) have been measured.[1] The spectra change somewhat as a function of coverage, with Cp vibrations only observed at low Fc pressures. This is consistent with the DFT mechanism which predicts that decomposition only occurs at step edges, with transport of Fc to the step edges being inhibited when a densely packed Fc adlayer forms. The calculations also predict that various low-energy approach structures such as **1** – **3** are likely, and indeed at high coverage differently oriented Fc are observed.[1] To investigate the possibility that structural information as a function of coverage can be obtained from HREELS, the molecular vibration frequencies for **1** – **3** were calculated. However, only small changes in frequencies are predicted, changes less than the observed changes attributed to diminishing Cp production with increasing coverage.

Significance for molecular-electronic devices. To appreciate the significance of this process for molecular-electronic devices, we consider a commonly made[11] junction formed using Au(111), chemisorbed ferrocenyl undecanethiol, and Pt(111), see Fig. 4. In such experiments there are many variables, including the coverage and the nature of the Au-S binding,[29-32] features that modify the details of key junction properties such as the magnitude of the conductivity and degree of rectification. Such details are not of concern here; instead we focus on the chemical processes that may occur involving the Pt(111) surface and the Fc tail group. However, we chose to work on a low coverage SAM that is sufficiently flexible to allow the alkane chain to be squashed to lie parallel to the metal surfaces (Fig. 4a-b), optimal vertically aligned chains (Fig. 4c-d), and kinked vertically aligned chains that present the Fc alternatively aligned to the Pt (Fig. 4e-h).

The strongest binding (of the thiyl form of the adsorbate molecule[30]) to the two electrode surfaces is found for the lying-down configurations shown in Fig. 4a-b, owing to the strong interactions that occur between the alkyl chain and the metals. A chemisorbed structure with H bridging Fe and Pt (Fig. 4a) is found to be 0.93 eV lower in energy than the corresponding physisorbed one (Fig. 4b). The chemisorbed structure is also predicted to be twice as conductive. The corresponding structures in which the adsorbate molecules stand up as in a typical[13] high-coverage alkanethiol SAM on Au(111), Fig. 4c-d, also have the chemisorbed structure being predicted to be more conductive, this time by a factor of 5. However, the conductivities are reduced by 6 orders of magnitude compared to the lying-down molecules, owing to the need for the current to tunnel through the alkane chain. The lowest-energy structure found for upright molecules is shown in Fig. 4e and has the alkyl chain kinked so as to present the opposite side of the Fc to the Pt surface, forming a stronger chemisorption bond but an order-of-magnitude less conductive linkage. Other chemisorbed variants conduct even more poorly, with the high-energy physisorbed variant conducting better in this case.

The calculations thus indicate that the conductivity of gold-alkylferrocene-platinum junctions is strongly dependent on the atomic details, including whether or not chemisorption occurs. If junctions are made passively by bringing Pt(111) up to established SAMs, then the upper junction structure may likely resemble the chemisorbed one in Fig. 4c, but if break-junction technologies are used or nanocrystalline electrodes of uncertain shape and orientation, then many other possibilities could occur.

Ferrocene-Pt(111) chemisorption is likely to be involved in the junctions thought to remain operative[11] up to an astonishing 520 GHz. For these, the measured conductivities are 0.011 G_0/nm^2, also astonishingly high for junctions involving long alkyl-chain molecules. The calculated conductivities for upright chains are at least 4 orders of magnitude less conductive than this, whereas if the connections on irregularly shaped contacts is actually dominated by a small number of chemisorbed molecules laying down as in Fig. 4a, then the observed results could easily be understood. At high coverage, the laying-down SAMs have about half the density as do the SAMs of upright chains.

CONCLUSIONS

The recent discovery[1] that, contrary to expectations based on the legendary stability of ferrocene on platinum electrodes in solution electrochemistry,[2-4] ferrocene spontaneously decomposes on contact with Pt(111) at low pressure in the gas phase, is understood using basic chemical theory in terms of two events. The first is chemisorption in which a Pt-C bond forms as well as a ferrocenium hydride, leading to a Fc-H-Pt bridge; this process could be in equilibrium with physisorbed π-stacked ferrocene. Second, the adsorbed species diffuse to step edges where hydrogen catalyzes the unfolding of the Fc sandwich to leave separated, chemisorbed, Cp rings and Fe atoms.

When the Fc is tethered to a SAM, the binding of it to its tether will control the range of angles at which the Fc can approach a Pt(111) surface. Intermolecular packing forces as a function of coverage will also affect this. In principle, all eight structures shown in Fig. 4 would seem to be feasible under appropriate conditions in some break-junction experiment in which the location and orientation of the Pt(111) surface is controlled. Alternatively, the Pt could take on a tip-like structure rather than the envisaged flat structures used herein, structures naively expected to be more reactive. The results in Fig. 4 suggest that chemisorption, at least to the stage of **3** wherein a Pt-C bond forms to a ferrocenium hydride, will always need to be considered in molecular-electronics experiments of Fc approaching Pt(111), especially at low coverage. This should enhance conductivity by a small but significant factor of order times 2 to 5, requiring the reinvestigation of observed phenomena on Pt(111) – Fc junctions.[11] However, as the

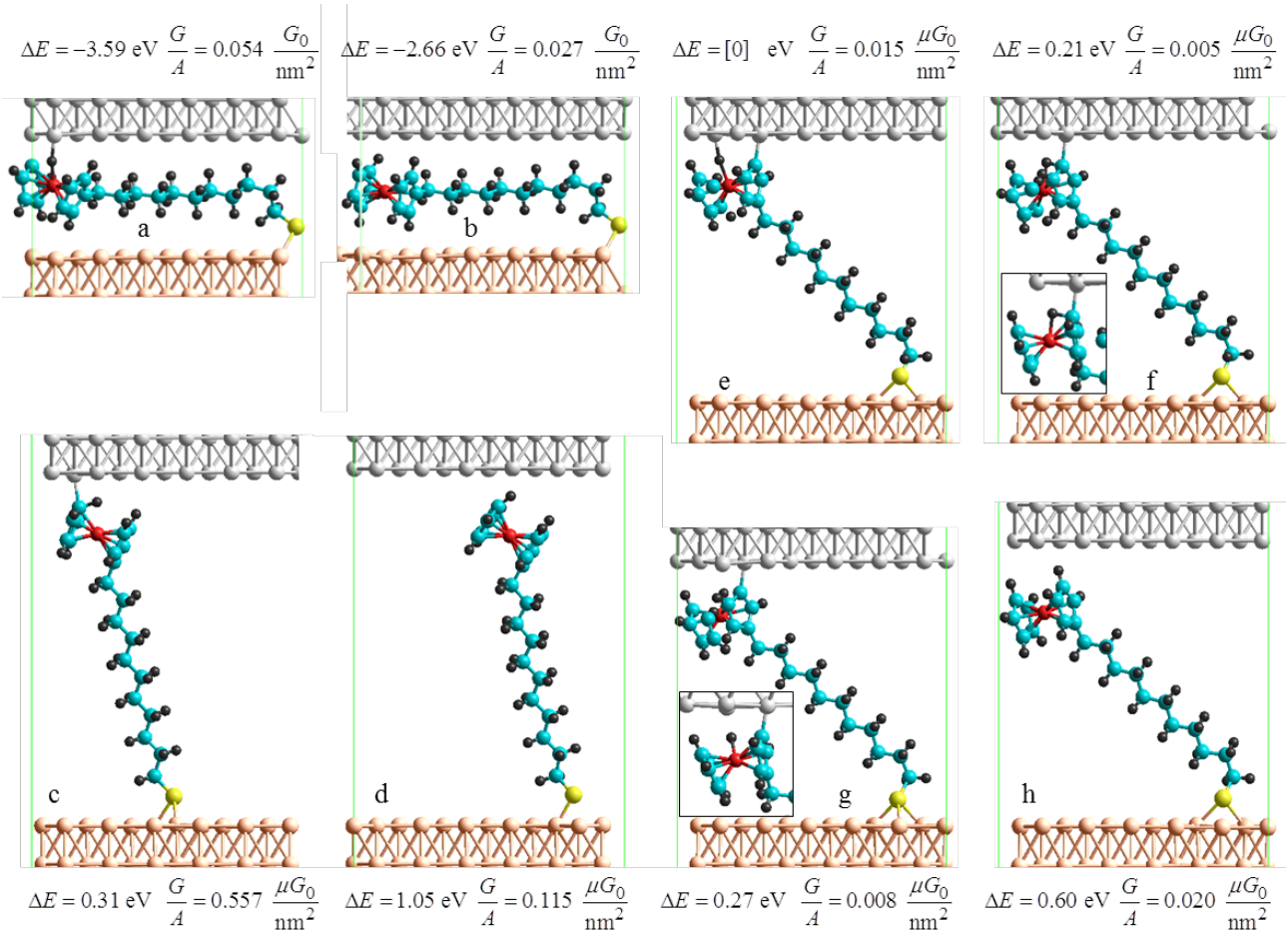

Figure 4. Ferrocenyl undecanethiol SAMs on Au(111) contacted by at Pt(111) surface. Conductance values are listed per unit area of analogous high-coverage SAMs, coverages of 2.7 molecules/nm^2 for c-h[11, 18] and 1.3 molecules/nm^2 for a-b; observed value in SAM rectifiers[11] is $G/A = 0.011\ G_0$/nm^2. Au- orange, Pt- white, Fe- red, S- yellow, C- cyan, H- black, box-vectors- green.

Fc motions depicted in Fig. 2 are sizeable, it is likely that tethering of the Fc will inhibit its decomposition reaction, even if the Pt is irregular enough so as to present catalytic sites. Such basic and reversible chemisorption alone. in high-density upright SAM structures, is shown to be insufficient to explain the factor of 10^4 discrepancy between the expected and observed[11] conductivity of some gold-alkanethiol-ferrocene-platinum junctions with extremely high rectification cut-off frequencies. Instead, the discrepancy could be understood by envisioning a SAM of about half the maximum monolayer coverage in which the molecular layer is squashed between the two metal surfaces.

ASSOCIATED CONTENT

Supporting Information

Provided are technical descriptions of the NANODCAL calculations plus listing of all structures either presented in the figures or else required to deduce the presented energies.

AUTHOR INFORMATION

Corresponding Author

Jeffrey.reimers@shu.edu.cn, Jeffrey.Reimers@uts.edu.au, Daniel.Kosov@jcu.edu.au.

Notes

The authors declare no competing financial interests.

ACKNOWLEDGMENT

We thank the National Natural Science Foundation of China (NSFC; Grant No. 11674212, as well as National Computational Infrastructure (NCI) and the Shanghai High-End Foreign Talents Programme for supporting this research.

REFERENCES

1. Paul, R.; Reifenberger, R. G.; Fisher, T. S.; Zemlyanov, D. Y., Atomic Layer Deposition of Feo on Pt(111) by Ferrocene Adsorption and Oxidation. *Chem. Mater.* **2015**, *27*, 5915-5924.

2. Gritzner, G.; Kuta, J., International Union of Pure and Applied Chemistry Physical Chemistry Division Commission on Electrochemistry Recommendations on Reporting Electrode Potentials in Nonaqueous Solvents. *Pure Appl. Chem.* **1984**, *56*, 461-466.

3. Malpas, R. E., The Electrochemistry and Photoelectrochemistry of an Aqueous Ferrocene/Ferricenium Redox Couple at Platinum, N-Silicon and N-Indium Phosphide Electrodes. *J. Electrochem. Soc.* **1982**, *129*, 1987-1993.

4. Zara, A. J.; Machado, S. S.; Bulhões, L. O. S.; Benedetti, A. V.; Rabockai, T., The Electrochemistry of Ferrocene in Non-Aqueous Solvents. *J. Electroanal. Chem.* **1987**, *221*, 165-174.

5. Özdamar, B.; Massobrio, C.; Boero, M., Stability and Destabilization Processes in the Formation of Ferrocene-Based Metal–Organic Molecule–Metal Nano-Junctions. *J. Phys. Chem. C* **2016**, *120*, 13825-13830.

6. Nijhuis, C. A.; Reus, W. F.; Barber, J. R.; Dickey, M. D.; Whitesides, G. M., Charge Transport and Rectification in Arrays of Sam-Based Tunneling Junctions. *Nano Lett.* **2010**, *10*, 3611-3619.

7. Nijhuis, C. A.; Reus, W. F.; Siegel, A. C.; Whitesides, G. M., A Molecular Half-Wave Rectifier. *J. Am. Chem. Soc.* **2011**, *133*, 15397-15411.

8. Nerngchamnong, N.; Yuan, L.; Qi, D.-C.; Li, J.; Thompson, D.; Nijhuis, C. A., The Role of Van Der Waals Forces in the Performance of Molecular Diodes. *Nat Nano* **2013**, *8*, 113-118.

9. Jeong, H., et al., Redox-Induced Asymmetric Electrical Characteristics of Ferrocene- Alkanethiolate Molecular Devices on Rigid and Flexible Substrates. *Adv. Funct. Mater.* **2014**, *24*, 2472-2480.

10. Metzger, R. M., Quo Vadis, Unimolecular Electronics? *Nanoscale* **2018**, *10*, 10316-10332.

11. Trasobares, J.; Vuillaume, D.; Théron, D.; Clément, N., A 17 Ghz Molecular Rectifier. *Nat. Commun.* **2016**, *7*, 12850.

12. Chen, X.; Roemer, M.; Yuan, L.; Du, W.; Thompson, D.; Del Barco, E.; Nijhuis, C. A., Molecular Diodes with Rectification Ratios Exceeding 105 Driven by Electrostatic Interactions. *Nat. Nanotechnol.* **2017**, *12*, 797-803.

13. Thompson, D.; Nijhuis, C. A., Even the Odd Numbers Help: Failure Modes of Sam-Based Tunnel Junctions Probed Via Odd-Even Effects Revealed in Synchrotrons and Supercomputers. *Acc. Chem. Res.* **2016**, *49*, 2061-2069.

14. Yuan, L.; Breuer, R.; Jiang, L.; Schmittel, M.; Nijhuis, C. A., A Molecular Diode with a Statistically Robust Rectification Ratio of Three Orders of Magnitude. *Nano Lett.* **2015**, *15*, 5506-5512.

15. Jeong, H.; Kim, D.; Xiang, D.; Lee, T., High-Yield Functional Molecular Electronic Devices. *ACS Nano* **2017**, *11*, 6511-6548.

16. Tian, H.; Dai, Y.; Shao, H.; Yu, H. Z., Modulated Intermolecular Interactions in Ferrocenylalkanethiolate Self-Assembled Monolayers on Gold. *J. Phys. Chem. C* **2013**, *117*, 1006-1012.

17. Fujii, S.; Kurokawa, S.; Murase, K.; Lee, K.-H.; Sakai, A.; Sugimura, H., Self-Assembled Mixed Monolayer Containing Ferrocenylthiol Molecules: Stm Observations and Electrochemical Investigations. *Electrochim. Acta* **2007**, *52*, 4436-4442.

18. Nijhuis, C. A.; Reus, W. F.; Whitesides, G. M., Molecular Rectification in Metal−Sam−Metal Oxide−Metal Junctions. *J. Am. Chem. Soc.* **2009**, *131*, 17814-17827.

19. Taylor, J.; Guo, H.; Wang, J., *Ab Initio* Modeling of Quantum Transport Properties of Molecular Electronic Devices. *Phys. Rev. B* **2001**, *63*, 245407.

20. Kresse, G.; Hafner, J., Ab Initio Molecular Dynamics for Liquid Metals. *Phys. Rev. B* **1993**, *47*, 558-561.

21. Kresse, G.; Joubert, D., From Ultrasoft Pseudopotentials to the Projector Augmented-Wave Method. *Phys. Rev. B* **1999**, *59*, 1758.

22. Perdew, J. P.; Burke, K.; Ernzerhof, M., Generalized Gradient Approximation Made Simple. *Phys. Rev. Lett.* **1996**, *77*, 3865-3868.

23. Goerigk, L.; Grimme, S., A Thorough Benchmark of Density Functional Methods for General Main Group Thermochemistry, Kinetics, and Noncovalent Interactions. *Phys. Chem. Chem. Phys.* **2011**, *13*, 6670-6688.

24. Oliver, D. J.; Maassen, J.; El Ouali, M.; Paul, W.; Hagedorn, T.; Miyahara, Y.; Qi, Y.; Guo, H.; Grutter, P., Conductivity of an Atomically Defined Metallic Interface. *Proc. Natl. Acad. Sci. U. S. A.* **2012**, *109*, 19097-19102.

25. Frisch, M. J., et al., *Gaussian 16*; Gaussian Inc.: Wallingford, CT, 2016.

26. Becke, A. D., Density-Functional Thermochemistry. Iii. The Role of Exact Exchange. *J. Chem. Phys.* **1993**, *98*, 5648-52.

27. Hehre, W. J.; Ditchfield, R.; Pople, J. A., Self-Consistent Molecular Orbital Methods. Xii. Further Extensions of Gaussian-Type Basis Sets for Use in Molecular Orbital Studies of Organic Molecules *J. Chem. Phys.* **1972**, *56*, 2257-61.

28. Hay, P. J.; Wadt, W. R., *J. Chem. Phys.* **1985**, *82*, 270 284 299.

29. Reimers, J. R.; Ford, M. J.; Marcuccio, S. M.; Ulstrup, J.; Hush, N. S., Competition of Van Der Waals and Chemical Forces on Gold–Sulfur Surfaces and Nanoparticles. *Nat. Rev. Chem.* **2017**, *1*, 0017.

30. Reimers, J. R.; Ford, M. J.; Halder, A.; Ulstrup, J.; Hush, N. S., Gold Surfaces and Nanoparticles Are Protected by Au(0)-Thiyl Species and Are Destroyed When Au(I)-Thiolates Form. *Proc. Natl. Acad. Sci. U.S.A.* **2016**, *113*, E1424-E1433.

31. Wang, Y.; Chi, Q.-J.; Zhang, J.-D.; Hush, N. S.; Reimers, J. R.; Ulstrup, J., Chain-Branching Control of the Atomic Structure of Alkanethiol-Based Gold-Sulfur Interfaces. *J. Am. Chem. Soc.* **2011**, *133*, 14856-14859.

32. Inkpen, M. S.; Liu, Z. F.; Li, H.; Campos, L. M.; Neaton, J. B.; Venkataraman, L., Non-Chemisorbed Gold–Sulfur Binding Prevails in Self-Assembled Monolayers. *Nat. Chem.* **2019**, *11*, 351-358.

TOC Graphic

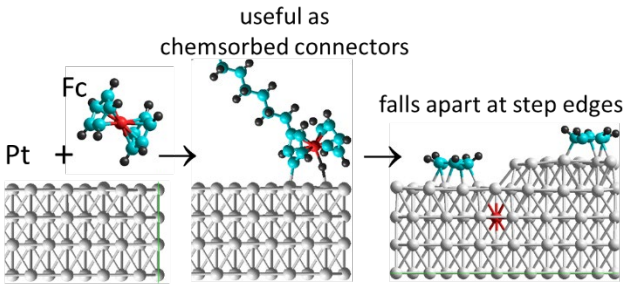
useful as
chemsorbed connectors
Fc
Pt
+
falls apart at step edges